

Synthesis and Evaluation of Oxyguanidine Analogues of the Cysteine Protease Inhibitor WRR-483 against Cruzain

Brian D. Jones,^{†,○} Anna Tochowicz,^{‡,○} Yinyan Tang,[§] Michael D. Cameron,^{||} Laura-Isobel McCall,[⊥] Ken Hirata,[#] Jair L. Siqueira-Neto,[⊥] Sharon L. Reed,[▽] James H. McKerrow,^{‡,◆} and William R. Roush^{*,†}

[†]Department of Chemistry, The Scripps Research Institute, 130 Scripps Way, Jupiter, Florida 33458, United States

[‡]Department of Pathology and Sandler Center for Drug Discovery, University of California-San Francisco, 1700 Fourth Street, San Francisco, California 94158-2250, United States

[§]Small Molecule Discovery Center, University of California-San Francisco, 1700 Fourth Street, San Francisco, California 94158-2250, United States

^{||}Department of Molecular Therapeutics, The Scripps Research Institute, 130 Scripps Way, Jupiter, Florida 33458, United States

[⊥]Skaggs School of Pharmacy and Pharmaceutical Sciences, University of California-San Diego, 9500 Gilman Drive, La Jolla, California 92093, United States

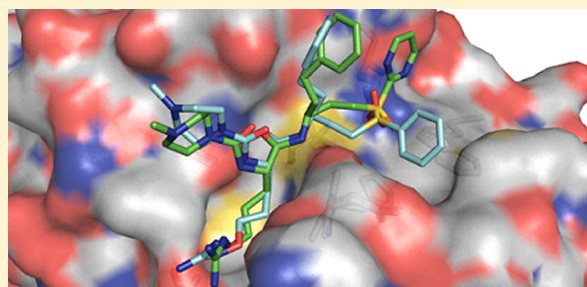
[#]Department of Pathology, University of California-San Diego, 9500 Gilman Drive, La Jolla, California 92093, United States

[▽]Departments of Pathology and Medicine, University of California-San Diego, 9500 Gilman Drive, La Jolla, California 92093, United States

Supporting Information

ABSTRACT: A series of oxyguanidine analogues of the cysteine protease inhibitor WRR-483 were synthesized and evaluated against cruzain, the major cysteine protease of the protozoan parasite *Trypanosoma cruzi*. Kinetic analyses of these analogues indicated that they have comparable potency to previously prepared vinyl sulfone cruzain inhibitors. Co-crystal structures of the oxyguanidine analogues WRR-666 (4) and WRR-669 (7) bound to cruzain demonstrated different binding interactions with the cysteine protease, depending on the aryl moiety of the P₁' inhibitor subunit. Specifically, these data demonstrate that WRR-669 is bound noncovalently in the crystal structure. This represents a rare example of noncovalent inhibition of a cysteine protease by a vinyl sulfone inhibitor.

KEYWORDS: Chagas' disease, cysteine protease inhibitor, X-ray crystallography, kinetics, vinyl sulfone, noncovalent inhibitor



The parasitic organism *Trypanosoma cruzi* is the causative agent of Chagas' disease, which affects millions of people mostly in the American continent, from Argentina to the southern US.^{1,2} Chagas' disease is considered a neglected tropical disease (NTD) with inadequate therapy and emerging drug resistance. Patients are usually poor people in rural areas, and only recently have major pharmaceutical companies invested in initiatives targeting drug development for Chagas' disease. Aside from transmission by blood-sucking insect vector known as the kissing-bug, there is a risk of infection through blood transfusion, congenital transmission from infected mother to child, consumption of contaminated food or drink, and organ donation.² Due to increased international travel and immigration patterns, spread of the disease has been observed over the last two decades to previously nonendemic regions including Europe, Japan, and Australia.

The current drug therapies for Chagas' disease, benznidazole and nifurtimox, are inadequate in terms of efficacy and toxicity.^{3,4} Both medicines are effective in curing the disease

only if given soon after infection, at the onset of the acute phase.⁵ Recent clinical trials demonstrated the inability of benznidazole to prevent progression of cardiomyopathy in chronic phase patients.⁶ Several new targets are the subject of ongoing research for the development of anti-Chagas agents.^{7,8}

Cruzain, a critical cysteine protease of *T. cruzi*, is a drug target for Chagas disease.⁹ Efficacy of the vinyl sulfone inhibitors K-11777 (1) and WRR-483 (2) (Figure 1) against cruzain in mouse^{10,11} and dog¹² models of Chagas' disease have been demonstrated. Previous studies indicated that WRR-483 (2) is also highly active against EhCP1,¹³ a virulence factor of *Entamoeba histolytica*.

As part of our ongoing efforts to develop an effective therapy for Chagas' disease, we have developed and report herein the synthesis of new oxyguanidine mimics of WRR-483 (2), kinetic

Received: August 14, 2015

Accepted: December 7, 2015

Published: December 15, 2015

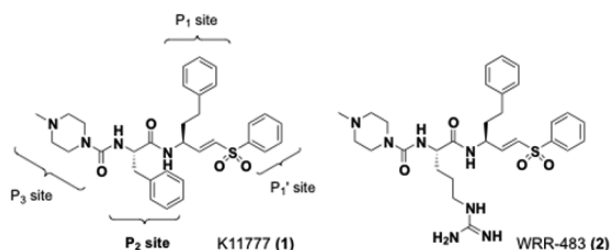


Figure 1. Structures of cysteine protease inhibitors K11777 (**1**) and WRR-483 (**2**).

studies evaluating their potency against cruzain, and cocrystal structures of cruzain in complex with WRR-666 (**4**) and WRR-669 (**7**).

Inhibitor Development and Synthesis. The current effort began in an attempt to generate analogues of **2** that would have favorable PK properties (**2** is not orally bioavailable). Accordingly, several previously described guanidine mimics with reduced basicity¹⁴ were incorporated into the P₂ site. Among the WRR-483 analogues evaluated, oxyguanidine derivatives WRR-662 (**3**) and WRR-666 (**4**) showed the most promising activity as cruzain inhibitors. Inhibitor WRR-667 (**5**) with P₂ = homoArg was also synthesized as a control. WRR-668 and WRR-669 (**6–7**) are analogues with pyridinyl and pyrimidinyl P₁' vinyl sulfone substituents, respectively (Figure 2). The pyridinyl and pyrimidinyl vinyl sulfone inhibitors were included because the aryl unit is known to influence the Michael reactivity of the vinyl sulfone.^{15–17}

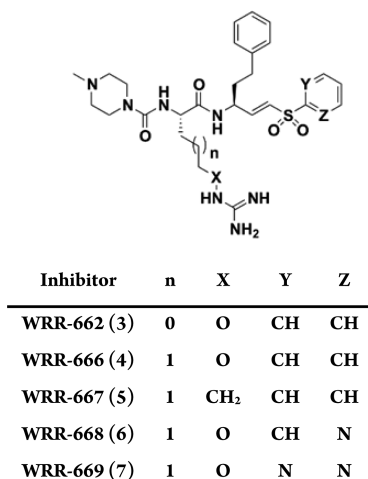
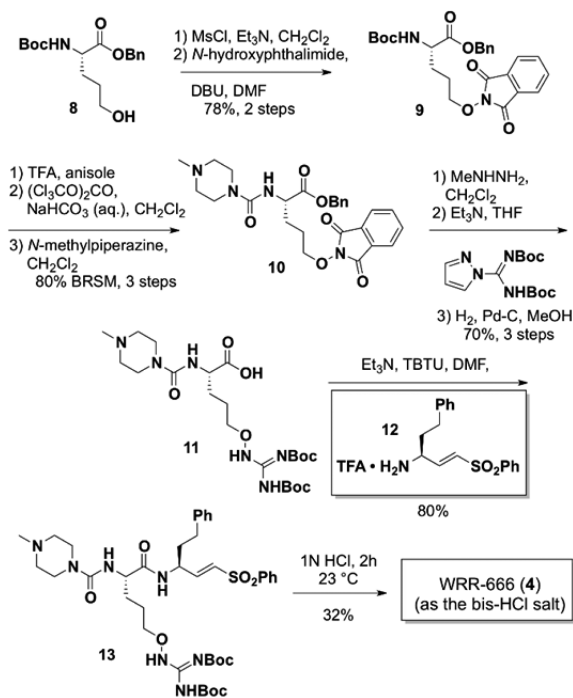


Figure 2. Structures of oxyguanidine analogues of WRR-483 (**2**) evaluated in this study, plus reference control compound WRR-667 (**5**).

These inhibitors were synthesized using a combination of methods previously utilized for synthesis of dipeptidyl vinyl sulfones,^{15,18,19} together with known methods of oxyguanidine synthesis.^{20,21} The synthesis of WRR-666 (**4**) is representative (Scheme 1). *N*-Boc-L-glutamic acid α -benzyl ester was reduced to the primary alcohol **8**,²² which was then converted to the phthalimidooxy derivative **9** via displacement of the derived mesylate with *N*-hydroxyphthalimide. Cleavage of the *tert*-butoxy-carbonyl protecting group provided the amino ester, which was converted to the *N*-methylpiperazine urea **10** by sequential treatment with triphosgene and *N*-methylpiperazine.²³ Elaboration of **10** to the protected oxyguanidine **11** was

Scheme 1. Synthesis of WRR-666 (**4**)



effected by phthalimide cleavage using *N*-methylhydrazine and treatment of the free *N*-alkoxyamine intermediate with *N,N'*-diboc guanylpiperazine.²⁴ Hydrogenolysis of the benzyl ester and standard peptide coupling of the resulting acid **11** with amine **12**¹¹ provided **13**, which was directly converted to the HCl salt of **4** by removal of the Boc protecting groups with aqueous HCl. Intermediate acid **11** was used in the synthesis of analogues **6** and **7**, which have heteroaryl P₁' vinyl sulfone units (see Supporting Information for details).

Recognizing that the weak N–O bonds of “internal” oxyguanidines **3–4** and **6–7** might be subject to reductive cleavage *in situ*,^{25,26} several inhibitors with an *N*-methoxyl group “external” to the guanidinium unit were designed (Figure 3). In addition, if the N–O bond were to undergo reductive cleave *in vivo*, the resulting cleavage products would be highly active inhibitors of cruzain (e.g., **2** in the case of **14**).

Analogues **14** and **15** were synthesized from the orthogonally protected ornithine derivative **17** using appropriate modifica-

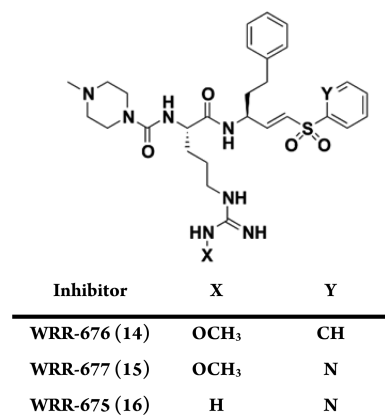
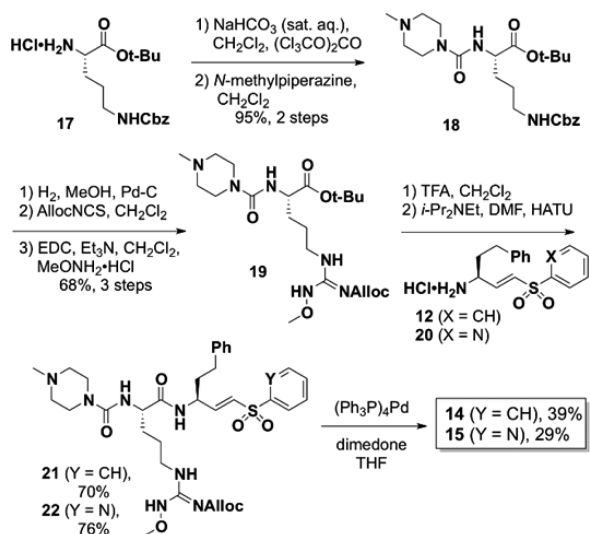


Figure 3. Structures of “external” oxyguanidines **14–15** and reference control inhibitor **16**.

tions of a known method for generating protected N^G -hydroxyguanidines (Scheme 2).²⁷ Key to the success of this

Scheme 2. Synthesis of External Oxyguanidines 14 and 15



synthesis was the ability to protect the amine generated by hydrogenolysis of 18 with AllocNCS to generate the Alloc-protected *N*-alkoxy-guanidine derivative 19. AllocNCS was generated from allyl chloroformate and potassium thiocyanate using the reported procedure for preparation of CbzNCS.²⁷ Completion of the syntheses of 14 and 15 were accomplished by standard coupling of the carboxylic acid derived from 19 with the γ -aminovinylsulfones 12 and 20 followed by Pd(0)-mediated deprotection of the Alloc protecting group.^{28,29}

Kinetic Data for Inhibition of Cruzain. Results of *in vitro* kinetic assays of the inhibitors generated in this study vs cruzain are shown in Table 1. The vast majority of these compounds

Table 1. Kinetic Constants for Inhibition of Cruzain by the Oxyguanidine Inhibitors

inhibitor	k_{inact}/K_i ($\text{s}^{-1} \text{M}^{-1}$) (pH = 5.5)	k_{inact}/K_i ($\text{s}^{-1} \text{M}^{-1}$) (pH = 8.0)
3	93100	138200
4	43300	53400
5	11000	59700
6	213800	308000
7	320400	1500 ^a
14	9100	65700
15	25000	1167800
16	8100	3100 ^a
1 ^b	158400	32500
2 ^b	36600	113200

^a $K_{\text{obs}}/[i]$ values ^bKinetic constants for 1 and 2 determined in this study do not agree with previously published values.¹¹ Although the kinetic assay protocol was the same, the cruzain used was from an alternative preparation (see SI).

were more potent than WRR-483 (2) as inhibitors of cruzain at pH = 5.5, while three (3, 6, and 15) were significantly more active at pH = 8. Based on these data, the inhibitors can be organized into three groups: (1) those with pH independent inhibition, including oxyguanidines 3 (WRR-662), 4 (WRR-666), 6 (WRR-668), and 16 (WRR-675); (2) those that are significantly more active (≥ 3 -fold) at pH = 8.0 compared to pH

= 5.5 [e.g., 5 (WRR-667), 14 (WRR-676), 15 (WRR-677), and 2 (WRR-483)]; and (3) those that are significantly more active (≥ 5 fold) at pH = 5.5 compared to at pH = 8.0. The latter category includes compounds 1 (K11777) and 7 (WRR-669). The data for inhibitor 7 (WRR-669) are particularly striking, as the second order rate of inhibition of cruzain is significantly greater at pH 5.5 than at pH 8.0. This suggests a most unusual mode of inhibition occurs with 7 and is one of the reasons that its cocrystal structure with cruzain was solved (*vide infra*).

In Vitro and in Vivo Assessment of Selected Inhibitors. The stability of analogues 4, 6, 14, and 15 to hepatic microsomes (human, rat, and mouse) were evaluated relative to the control compounds 1 and 2 (Table S2, Supporting Information). These data demonstrate that analogues 6 and 15 had substantially improved microsomal stability relative to 1 and 2. None of the analogues tested showed significant inhibition of CYP enzymes involved in drug metabolism (1A2, 2C9, 2D6, and 3A4) (Table S3).

In vivo pharmacokinetic studies were conducted with several of these analogues (Table S4). Unfortunately, these data showed that none of these analogues had PK properties superior to WRR-483. Preliminary IP dosing of analogue 6 in mice also indicated that this compound was cleared more rapidly than 2 or 4, with significantly lower plasma concentrations at all time points (Table S5). These data led us to speculate that the poor exposure of these compounds *in vivo* might be due to rapid reductive cleavage of the weak N–O bonds.

A metabolite ID study was conducted on analogue 6 to determine if it was reductively cleaved *in vivo* (Table S6). Metabolite 23 was observed at all time points, which confirmed this mode of metabolism was at least partially contributing to the suboptimal PK properties of the internal oxyguanidine analogues in rats (Figure 4).

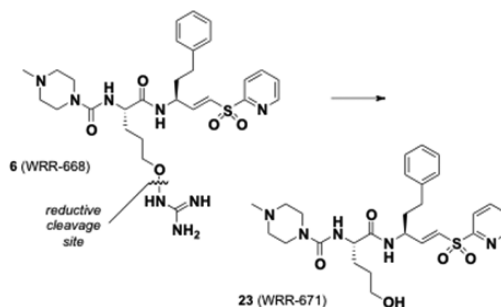


Figure 4. Metabolism of WRR-668 (6) by reductive N–O bond cleavage.

A study of the stability of analogue 15 in mouse plasma in the presence and absence of EDTA indicated that this compound is cleaved proteolytically by a metallo-enzyme (Figure S1, Supporting Information).

The antiparasitic activity of inhibitor 14 was evaluated with *T. cruzi* infected macrophage cells, resulting in an EC_{50} value of 269 nM. This set of inhibitors were also tested against *E. histolytica* cysteine protease 1 (EhCP1), and several (including 6, 15 and 16) were found to be low nM inhibitors of this protease (Table S7).

X-ray Crystal Structures of Cruzain with Bound 4 and 7. The crystal structures of cruzain complexes with WRR-666 (4) at 1.2 Å resolution and WRR-669 (7) with 2.5 Å resolution were obtained (Table S1). The overall structures are similar to

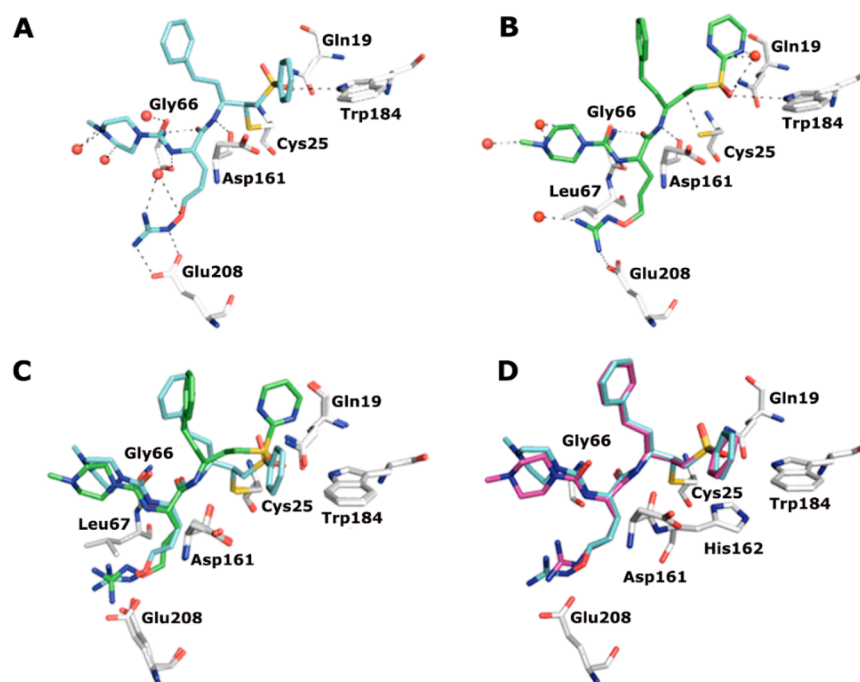


Figure 5. View of cruzain active sites with bound inhibitors. (A) Crystal structure of cruzain (gray carbons) bound to WRR-666 (4) (blue carbons) and (B) cruzain (gray carbons) bound to WRR-669 (7) (green carbons). Water mediated hydrogen bonds connecting the inhibitors to the protein are shown as black dashes. Crystallographic water molecules involved in the network are depicted as red spheres. (C) Superimposition of both crystal structures, complexes of cruzain with 4 and 7. (D) Superimposition of complexes of cruzain–4 (blue carbons) and WRR-483 (2) (magenta carbons).

those previously reported for cruzain with bound vinyl sulfone inhibitors,^{11,30} in that they fold into two distinct domains with the active site positioned between them. The complex with 4 was in a monoclinic crystal form (C121) with two molecules in the asymmetric unit (AU), as previously observed for complexes with K11777 (1) (PDB ID: 2OZ2) and WRR-483 (2) (PDB ID: 3LXS). However, the cruzain–7 complex formed a hexagonal crystal form (P32) with three molecules very differently packed within the asymmetric unit, compared with all previously reported cruzain structures.

A covalent adduct of the inhibitor with catalytic Cys 25 was observed in the cruzain–4 complex, as deduced by the cysteine–sulfur and inhibitor C(4) carbon distance of 1.9 Å (in both molecules A and B, respectively) (Figure 5A). However, there is no covalent bond between the inhibitor and Cys 25 in the cruzain–7 structure (the average C–S bond distance between is 3.2 Å) (Figure 5B). In each complex, a conserved system of polar interactions is observed between protein and inhibitor associated through Gln19, Gly66, Asp161, and Trp184. These interactions serve primarily to anchor the peptidyl backbone of the inhibitor in the cruzain active site.

The superimposed cruzain–4 (or 7) complex with the previously reported structure of WRR-483 (2) bound to cruzain illustrates similar interactions with the active site for the inhibitors (Figure 5D). Nonetheless, the vinyl sulfone moiety of 7 is turned about 90° toward Trp184 and the C=C remains intact (Figure 5C). The pyrimidyl ring of 7 is turned about 45° relative to the phenyl ring of 4 (Figure 5B,C) and others like 2 (Figure 5D) and is flipped toward P₂' site of the pocket.

In all three chains of the cruzain–7 complex, one of the vinyl sulfone oxygens forms a hydrogen bond with Gln19 (2.7 Å) and a hydrophobic interaction with Trp184 (3.4 Å). The second oxygen of the vinyl sulfone is coordinated by a water

molecule in chains A and B (3.2 Å) (Figure 5B). In chain A, the same water interacts with the N-2 from the pyrimidyl ring (2.7 Å) (Figure 5B). Moreover, in chain B, the pyrimidyl ring is rotated about 30° compared with its orientation in chains A and C.

The oxyguanidine mimic of the L-homoarginine residue inserted into the P₂ site of inhibitor 4 makes contacts as previously reported for the L-arginine P₂ analogue of K11777, WRR-483 (2). One of the terminal nitrogens (N16) of the guanidinium unit makes a hydrogen bond with Glu208 (3.3 Å), whereas a second guanidinium nitrogen N17 makes hydrogen bond with water molecule (2.7 Å). The same water molecule coordinates the oxyguanidine oxygen in 4 (Figure 5A). Hydrogen bonding interactions are also formed at the P₃ site between the N-methylpiperazine basic nitrogen and two water molecules (2.6 and 3.2 Å) (Figures 5A,B).

The crystal structure of the cruzain–7 complex that indicated noncovalent inhibition was an unexpected observation. Based on the kinetic data summarized in Table 1, we reasoned that the mode of inhibition of cruzain by compound 7 might be pH dependent. All the inhibitors reported here, with the single exception of 7, showed time-dependent inhibition at both pH 5.5 and 8.0. Indeed, the inhibition of cruzain by 7 at pH = 8.0 was not time dependent, whereas at pH = 5.5 time dependence was observed (data not shown). This represents a rare example of noncovalent inhibition of a cysteine protease by a vinyl sulfone inhibitor.³¹ The factors that cause inhibitor 7 to display this unusual reversible inhibition of cruzain remain to be determined, especially when the other inhibitors examined in this study do not.

The data reported here for internal oxyguanidine inhibitors 3–7 indicates that guanidine mimetics and side-chain length modification are tolerated in the WRR-483 inhibitor scaffold

with respect to *in vitro* potency vs cruzain. The external oxyguanidine inhibitors 14–15 also retain activity against cruzain despite structural modifications at P₂, implying some flexibility of the target at this position.

The cocrystal structures of inhibitors 4 and 7 bound to cruzain confirm previously observed interactions between the cruzain active site and related inhibitors, although the cruzain–7 complex and kinetic data at pH = 8 indicates reversibility of inhibition of cruzain by this inhibitor.

■ ASSOCIATED CONTENT

Supporting Information

The Supporting Information is available free of charge on the ACS Publications website at DOI: 10.1021/acsmmedchem-lett.5b00336.

Synthesis, experimental methods, and crystallographic data (PDF)

Accession Codes

Atomic coordinates and structure factors of the reported crystal structures have been deposited to the Protein Data Bank under accession codes 4PI3 and 4PI4.

■ AUTHOR INFORMATION

Corresponding Author

*E-mail: roush@scripps.edu.

Present Address

♦Skaggs School of Pharmacy and Pharmaceutical Sciences, University of California-San Diego, 9500 Gilman Drive, MC 0657, La Jolla, California 92093–0657, United States.

Author Contributions

○These authors contributed equally to this work. The manuscript was written through contributions of all authors. All authors have given approval to the final version of the manuscript.

Funding

This work was supported in part by National Institutes of Health (NIH) Grant UO1-AI077822

Notes

The authors declare no competing financial interest.

■ ABBREVIATIONS

Gln, glutamine; Gly, glycine; Trp, tryptophan; Asp, aspartic acid; Glu, glutamic acid; k_{obs} , observed rate constant; K_i , reversible inhibition constant; k_{inact} , apparent maximum inactivation rate constant; K_M , Michaelis–Menten constant; Boc, *tert*-butoxycarbonyl; Alloc, allyloxycarbonyl; IP, intraperitoneal; PK, pharmacokinetic; EDTA, *N,N'*-ethylenediaminetetraacetic acid; IV, intravenous; CYP, cytochrome P-450 enzyme

■ REFERENCES

- (1) Rassi, A., Jr.; Rassi, A.; Marin-Neto, J. A. Chagas disease. *Lancet* **2010**, 375, 1388–1402.
- (2) Wilson, L. S.; Strosberg, A. M.; Barrio, K. Cost-Effectiveness Of Chagas Disease Interventions In Latin America And The Caribbean: Markov Models. *Am. J. Trop. Med. Hyg.* **2005**, 73, 901–910.
- (3) Sajid, M.; Robertson, S.; Brinen, L.; McKerrow, J. Cruzain: the path from target validation to the clinic. In *Cysteine Proteases of Pathogenic Organisms*; Robinson, M.; Dalton, J., Eds.; Springer: New York, 2011; Vol. 712, pp 100–115.
- (4) Rodrigues Coura, J.; de Castro, S. L. A critical review on Chagas disease chemotherapy. *Mem. I. Oswaldo Cruz* **2002**, 97, 3–24.
- (5) Apt, W. Current and developing therapeutic agents in the treatment of Chagas disease. *Drug Des., Dev. Ther.* **2010**, 4, 243–253.
- (6) Morillo, C. A.; Marin-Neto, J. A.; Avezum, A.; Sosa-Estani, S.; Rassi, A.; Rosas, F.; Villena, E.; Quiroz, R.; Bonilla, R.; Britto, C.; Guhl, F.; Velazquez, E.; Bonilla, L.; Meeks, B.; Rao-Melacini, P.; Pogue, J.; Mattos, A.; Lazdins, J.; Connolly, S. J.; Yusuf, S. Randomized Trial of Benznidazole for Chronic Chagas' Cardiomyopathy. *N. Engl. J. Med.* **2015**, 373, 1295–1306.
- (7) Rivera, G.; Bocanegra-Garcia, V.; Ordaz-Pichardo, C.; Nogueira-Torres, B.; Monge, A. New Therapeutic Targets for Drug Design Against Trypanosoma cruzi, Advances and Perspectives. *Curr. Med. Chem.* **2009**, 16, 3286–3293.
- (8) Choi, J. Y.; Podust, L. M.; Roush, W. R. Drug Strategies Targeting CYP51 in Neglected Tropical Diseases. *Chem. Rev.* **2014**, 114, 11242–11271.
- (9) McKerrow, J. H. Development of cysteine protease inhibitors as chemotherapy for parasitic diseases: insights on safety, target validation, and mechanism of action. *Int. J. Parasitol.* **1999**, 29, 833–7.
- (10) Engel, J. C.; Doyle, P. S.; Hsieh, I.; McKerrow, J. H. Cysteine protease inhibitors cure an experimental Trypanosoma cruzi infection. *J. Exp. Med.* **1998**, 188, 725–34.
- (11) Chen, Y. T.; Brinen, L. S.; Kerr, I. D.; Hansell, E.; Doyle, P. S.; McKerrow, J. H.; Roush, W. R. In Vitro and In Vivo Studies of the Trypanocidal Properties of WRR-483 against Trypanosoma cruzi. *PLoS Neglected Trop. Dis.* **2010**, 4, e825.
- (12) Barr, S. C.; Warner, K. L.; Kornreic, B. G.; Piscitelli, J.; Wolfe, A.; Benet, L.; McKerrow, J. H. A cysteine protease inhibitor protects dogs from cardiac damage during infection by Trypanosoma cruzi. *Antimicrob. Agents Chemother.* **2005**, 49, 5160–1.
- (13) Melendez-Lopez, S. G.; Herdman, S.; Hirata, K.; Choi, M. H.; Choe, Y.; Craik, C.; Caffrey, C. R.; Hansell, E.; Chavez-Munguia, B.; Chen, Y. T.; Roush, W. R.; McKerrow, J.; Eckmann, L.; Guo, J.; Stanley, S. L., Jr.; Reed, S. L. Use of recombinant Entamoeba histolytica cysteine proteinase 1 to identify a potent inhibitor of amebic invasion in a human colonic model. *Eukaryotic Cell* **2007**, 6, 1130–6.
- (14) Masic, L. P. Arginine mimetic structures in biologically active antagonists and inhibitors. *Curr. Med. Chem.* **2006**, 13, 3627–3648.
- (15) Roush, W. R.; Gwaltney, S. L.; Cheng, J.; Scheidt, K. A.; McKerrow, J. H.; Hansell, E. Vinyl Sulfonate Esters and Vinyl Sulfonamides: Potent, Irreversible Inhibitors of Cysteine Proteases. *J. Am. Chem. Soc.* **1998**, 120, 10994–10995.
- (16) Reddick, J. J.; Cheng, J.; Roush, W. R. Relative Rates of Michael Reactions of 2'-(Phenethyl)thiol with Vinyl Sulfones, Vinyl Sulfonate Esters, and Vinyl Sulfonamides Relevant to Vinyl Sulfonamide Cysteine Protease Inhibitors. *Org. Lett.* **2003**, 5, 1967–1970.
- (17) Shenai, B. R.; Lee, B. J.; Alvarez-Hernandez, A.; Chong, P. Y.; Emal, C. D.; Neitz, R. J.; Roush, W. R.; Rosenthal, P. J. Structure-activity relationships for inhibition of cysteine protease activity and development of Plasmodium falciparum by peptidyl vinyl sulfones. *Antimicrob. Agents Chemother.* **2003**, 47, 154–60.
- (18) Roush, W. R.; Cheng, J. M.; Knapp-Reed, B.; Alvarez-Hernandez, A.; McKerrow, J. H.; Hansell, E.; Engel, J. C. Potent second generation vinyl sulfonamide inhibitors of the trypanosomal cysteine protease cruzain. *Bioorg. Med. Chem. Lett.* **2001**, 11, 2759–2762.
- (19) Gennari, C.; Salom, B.; Potenza, D.; Williams, A. Synthesis of Sulfonamido-Pseudopeptides: New Chiral Unnatural Oligomers. *Angew. Chem., Int. Ed. Engl.* **1994**, 33, 2067–2069.
- (20) Liu, F.; Thomas, J.; Burke, T. R. Synthesis of a homologous series of side-chain-extended orthogonally protected aminoxy-containing amino acids. *Synthesis* **2008**, 2008, 2432–2438.
- (21) Tomczuk, B.; Lu, T. B.; Soll, R. M.; Fedde, C.; Wang, A. H.; Murphy, L.; Crysler, C.; Dasgupta, M.; Eisenagel, S.; Spurlino, J.; Bone, R. Oxyguanidines: Application to non-peptidic phenyl-based thrombin inhibitors. *Bioorg. Med. Chem. Lett.* **2003**, 13, 1495–1498.
- (22) Broadrup, R. L.; Wang, B.; Malachowski, W. P. A general strategy for the synthesis of azapeptidomimetic lactams. *Tetrahedron* **2005**, 61, 10277–10284.

(23) Tsai, J. H.; Takaoka, L. R.; Powell, N. A.; Nowick, J. S. Synthesis of Amino Acid Ester Isocyanates: Methyl(S)-2-Isocyanato-3-Phenylpropionate. *Org. Synth.* **2002**, 78, 220.

(24) Konno, H.; Kubo, K.; Makabe, H.; Toshiro, E.; Hinoda, N.; Nosaka, K.; Akaji, K. Total synthesis of miraziridine A and identification of its major reaction site for cathepsin B. *Tetrahedron* **2007**, 63, 9502–9513.

(25) Kihara, H.; Prescott, J. M.; Snell, E. E. The bacterial cleavage of canavanine to homoserine and guanidine. *J. Biol. Chem.* **1955**, 217, 497–503.

(26) Takahara, K.; Nakanishi, S.; Natelson, S. Studies on the reductive cleavage of canavanine and canavaninosuccinic acid. *Arch. Biochem. Biophys.* **1971**, 145, 85–95.

(27) Martin, N. I.; Woodward, J. J.; Marletta, M. A. N-G-hydroxyguanidines from primary amines. *Org. Lett.* **2006**, 8, 4035–4038.

(28) Dangles, O.; Guibe, F.; Balavoine, G.; Lavielle, S.; Marquet, A. Selective cleavage of the allyl and (allyloxy)carbonyl groups through palladium-catalyzed hydrostannolysis with tributyltin hydride. Application to the selective protection-deprotection of amino acid derivatives and in peptide synthesis. *J. Org. Chem.* **1987**, 52, 4984–4993.

(29) Guibé, F. Allylic protecting groups and their use in a complex environment part II: Allylic protecting groups and their removal through catalytic palladium π -allyl methodology. *Tetrahedron* **1998**, 54, 2967–3042.

(30) Brinen, L. S.; Hansell, E.; Cheng, J.; Roush, W. R.; McKerrow, J. H.; Fletterick, R. J. A target within the target: probing cruzain's P1' site to define structural determinants for the Chagas' disease protease. *Structure* **2000**, 8, 831–40.

(31) Brak, K.; Doyle, P. S.; McKerrow, J. H.; Ellman, J. A. Identification of a new class of nonpeptidic inhibitors of cruzain. *J. Am. Chem. Soc.* **2008**, 130, 6404–10.

■ NOTE ADDED AFTER ASAP PUBLICATION

There was a spelling error in an author's name in the version published ASAP December 15, 2015; the corrected version was published ASAP on December 16, 2015.